Journal of Materials Chemistry C

Computational design of photoactive organic molecules for infrared responsive 2D perovskites

Journal:	*Journal of Materials Chemistry C*
Manuscript ID	TC-ART-04-2020-001807.R1
Article Type:	Paper
Date Submitted by the Author:	17-May-2020
Complete List of Authors:	Zalesny, Robert; Wroclaw University of Science and Technology, Department of Physical and Quantum Chemistry Alam, Md Mehboob; Universitetet i Tromso Kjemi, Chemistry Day, Paul; US Air Force Research Laboratory, RXAP Nguyen, Kiet ; US Air Force Research Laboratory, RXAP Pachter, Ruth; Air Force Research Laboratory, Materials & Manufacturing Directorate Lim, Chang-Keun; Nazarbayev University, School of Engineering and Digital Sciences Prasad, Paras; Institute for Lasers, Photonics, and Biophotonics, Ågren, Hans; KTH Royal Institute of Technology, Theoretical Chemistry and Biology

ARTICLE TYPE

Cite this: DOI: 10.1039/xxxxxxxxxx

Computational design of two-photon active organic molecules for infrared responsive materials†

Robert Zaleśny,*[a] Md. Mehboob Alam,[b] Paul N. Day,[c] Kiet A. Nguyen,[c] Ruth Pachter,[c] Chang-Keun Lim,[d,e] Paras N. Prasad,[d] Hans Ågren*[f]

Received Date
Accepted Date

DOI: 10.1039/xxxxxxxxxx

www.rsc.org/journalname

In this study we report theoretical studies of the linear and nonlinear optical properties of a series of π-conjugated organic cations and their neutral precursors which show π-stacking to exhibit aggregation-enhanced optical properties. These organic cations show promises as photoactive layers in hybrid quasi-2D perovskites for applications in optoelectronics, particularly in the short wavelength infrared region. We analyze one- and two-photon (2P) absorption (2PA) transition strengths of several excited states in the considered systems at the coupled-cluster level theory (employing CC2 model). Furthermore, a microscopic insight of their 2P activity has been obtained using the generalized few-state model (GFSM). Based on our GFSM results, we pinpoint the origin of the desired nonlinear optical properties and provide a design strategy for efficient IR photoactive organic materials with potential application in organic-inorganic hybrid quasi-2D perovskites.

1 Introduction

Nonlinear optical properties of molecular systems occupy privileged spot due to numerous potential technological applications which utilize optical limiting, all-optical switching, biomedical imaging using two-photon microscopy or data storage.[1–13] In particular, much effort has recently been put into development of design rules aiming at maximizing third-order nonlinearities. As far as these processes are concerned, two-photon absorption (2PA) is nowadays the most widely studied one.[14–20] It was predicted based on the perturbation theory by Maria Göppert-Mayer in 1931,[21] but the theory was confirmed experimentally 30 years later.[22,23] This third-order resonant process has a number of applications, e.g. it can be employed as a spectroscopic tool to identify symmetry-forbidden transitions[24] or to record Doppler-free spectra.[25] Potential technological applications of 2PA range from two-photon bio-imaging[4,5,26,27] to three-dimensional high density optical data storage.[1,2]

Another interesting application was demonstrated recently by some of the present authors who had introduced the concept of interlayer-sensitized photoluminescence of hybrid quasi-2D perovskite (PVSK) that incorporated an aggregation induced enhanced emission (AIEE) organic cation layer.[28] A rod-shaped AIEE organic cation (Z)-2-([1,1'-biphenyl]-4-yl)-3-(4-(3-aminopropoxy)phenyl)acrylonitrile, BPCSA+, and its neutral precursor BPCSA (Fig. 1) were synthesized to maximize energy sensitizing properties in the short wavelength IR region and to fit into the lattice of 3D PVSK layers. As demonstrated on the experimental basis, BPCSA+ emitted strong fluorescence in the solid state, while its solution was almost non-fluorescent. This clearly demonstrated the AIEE characteristic of BPCSA+. Upon incorporation into quasi-2D PVSKs as a bulky organic layer in between the 3D PVSK layers, BPCSA+ promoted the photoluminescence (PL) of PVSK up to 10 folds from that of non-π-conjugated organic cation (octylammonium) 2D PVSK. Importantly, BPCSA+ 2D PVSK displayed superior emission properties upon two-photon excitation by a short wavelength IR laser. As highlighted in the recent study, an AIEE sensitization system can reinforce the PL properties of PVSK upon linear/nonlinear optical excitations in PVSK based non-linear optical devices.

Following these encouraging experimental advances, in this study we aim at elucidating the photophysical properties of several π-conjugated organic cations (including their neutral precur-

[a] Department of Physical and Quantum Chemistry, Faculty of Chemistry, Wroclaw University of Science and Technology, Wybrzeże Wyspiańskiego 27, 50-370 Wrocław, Poland
[b] Department of Chemistry, Indian Institute of Technology Bhilai, Sejbahar, Raipur, Chhattisgarh – 492015, India
[c] Air Force Research Laboratory, Wright-Patterson Air Force Base, Dayton, OH, 45433 USA
[d] Institute for Lasers, Photonics, and Biophotonics, Department of Chemistry, University at Buffalo, State University of New York, Buffalo, NY, 14260 USA
[e] Department of Chemical and Material Engineering, School of Engineering and Digital Sciences, Nazarbayev University, Nur-Sultan City 010000, Kazakhstan
[f] Department of Theoretical Chemistry and Biology, School of Engineering Sciences in Chemistry, Biotechnology and Health, KTH Royal Institute of Technology, SE-106 91 Stockholm, Sweden
*E-mail: robert.zalesny@pwr.edu.pl (R.Z.), hagren@kth.se (H.Å.)

† Electronic Supplementary Information (ESI) available: geometries of studied complexes, numerical data corresponding to generalized-few state model calculations, simulated optical spectra. See DOI: 10.1039/cXCP00000x/

sors) shown in Fig. 1. These rod-shaped α-cyanostilbene derivatives have the potential to be AIEE active cations as well as to be used as photoactive layers in perovskites.[28] For the present study, besides the previously reported BPCSA, we designed three additional neutral precursors (NCSA, BMCSA, BPyMCSA) and theoretically studied the optical properties of their cationic (NCSA+) and dicationic (BMCSA+, BPyMCSA+) forms as well. To this end, we employ advanced electronic-structure methods to determine electronic spectra, including one- and two-photon transition strengths.

2 Computational details

The ground state geometries of the four neutral precursors (BPCSA, NCSA, BMCSA, BPyMCSA) shown in Fig. 1 and their cations (BPCSA+, NCSA+, BMCSA+, BPyMCSA+) were optimized using the density functional theoretical method with the B3LYP functional[29] and the cc-pVDZ basis set.[30] In doing so, we neglected environmental effects, i.e. we considered molecules in vacuo only. The minima on potential energy hypersurface were confirmed by evaluation of hessian. Subsequently, the minimum energy geometries were used for electronic-structure calculations. We performed the *ab initio* quantum-chemistry calculations using the resolution-of-identity coupled-cluster CC2 model[31] and the cc-pVDZ basis set. The choice of this method is dictated by recent reports that all studied density functional theory approximations show serious limitations as far as predictions of two-photon absorption strengths are concerned, i.e. hybrid functionals with fixed amount of HF exchange are burdened by cancellations of significant errors, while range-separated functionals systematically underestimate two-photon transition strengths due to their inability to correctly reproduce excited-state density distributions.[32,33] This is line with the results of calculations presented in ESI, where the comparison between CC2 and PBE0 and CAM-B3LYP is made. As far as the prediction of one-photon spectra is concerned, it should be highlighted that according to the benchmark work of Jacquemin *et al.*, one obtains a MAE of 0.27 eV for excitation energy of organic dyes at the CC2/TZVP level taking the CAS-PT2/TZVP level as the reference.[34] A similar level of accuracy is expected for the electronic excitation energies for molecules studied herein. Separately, the CC2 results for the four π-conjugated molecules were compared systematically to DFT/TD-DFT calculations. Such a comparison may assist in studying larger systems in future work. The results, also including solvent effects, are summarized in the ESI (see Tables S6-S9, Figures S1-S2). We conclude that in selection of the functional for calculation of 1PA, benchmarking with inclusion of solvent has to be considered. Moreover, the comparison of the calculated emission characteristics to experimental data demonstrated good agreement for BPCSA using the CAM-B3LYP functional. All the density functional theory calculations were performed with the GAUSSIAN 16 program,[35] while all the RI-CC2 calculations were carried out with the TURBOMOLE 7.3 program.[36] We used our own code for all the generalized few-state model (GFSM) calculations.

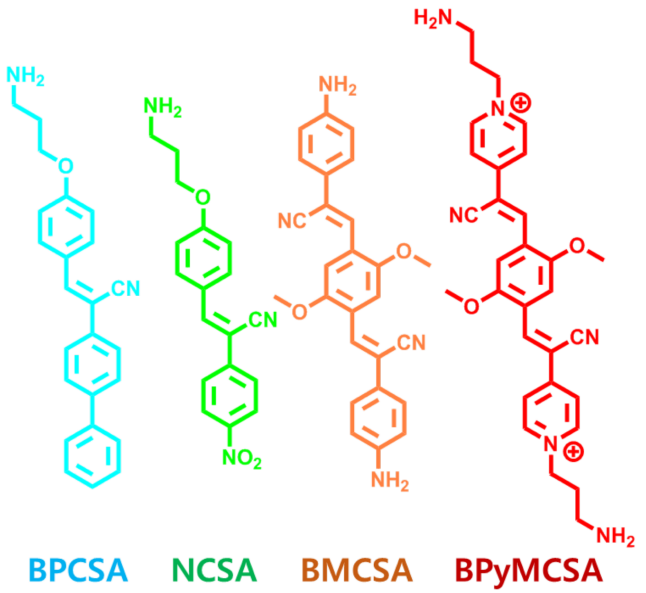

Fig. 1 Structures of precursors of photoactive cations studied in the present work. In the case of cations (denoted as BMCSA+, BPCSA+, BPyMCSA+, NCSA+), each -NH_2 group is replaced by -NH_3^+.

3 Results and Discussion

Based on our previous study on the AIEE cation sensitizing PL of its 2D PVSK composites,[28] we designed three more organic cation candidates which can form hybrid quasi-2D PVSKs (see Fig. 1). The rod-shaped cations, which have one-dimensional bulkiness, can facilitate 2D PVSK assembly by a well-fitted diameter matched to the 2D PVSK lattice size. The dipolar (NCSA) and quadrupolar (BMCSA+, BPyMCSA) structures, combining electron donor (D) and acceptor (A) groups to π-conjugation (NCSA: alkoxy(D)-nitro(A); BMCSA+: ammonium(A)-methoxy(D)-ammonium(A); BPyMCSA: pyridinium(A)-methoxy(D)-pyridinium(A)) can extend π-conjugation via intramolecular charge transfer (ICT) to improve their third-order nonlinear optical property.[37] In their 2D PVSK structures, mono ammonium cations (BPCSA+ and NCSA+) can form$(R\text{-}NH_3^+)_2MX_4$(R-NH3$^+$): alkyl or aryl ammonium cation; M: divalent metal cation (e.g. Pb^{2+}); X: halide), while diammonium cations (BMCSA+ and BPyMCSA+) can produce ($^+NH_3$-R-NH_3^+)MX_4.[38] The α-cyanostilbene framework can enhance PL of the candidates in the solid state (AIEE) by (i) restriction of energy dissipating rotational relaxation and (ii) formation of a head-to-tail molecular assembly (*J*-aggregation) to enlarge the Stokes shift, thus minimizing reabsorption of its own PL.[39] Potentially, this AIEE feature can improve one- and two-photon excited PL of their 2D PVSKs without any concentration quenching issue (significant PL quenching in the solid state or high concentration) faced by most organic luminophores. The structure of the four organic precursors considered in this work are shown in Fig. 1. The optimized coordinates are provided in Electronic Supplementary Information file.

3.1 One-photon absorption

The one-photon absorption is characterized by its oscillator strength (f), and the corresponding values for transitions from the ground state to the first five singlet excited states in all the four neutral and cationic precursors are presented in Table 1. The one-photon absorption spectra of all four neutral precursors share some common well-studied features. Firstly, the $S_0 \rightarrow S_1$ transition has very large oscillator strength indicating that they have the characteristics of a $\pi \rightarrow \pi^\star$ transition. Secondly, the extension of π-conjugated linker leads to a decrease of the excitation energy, e.g. on passing from NCSA to BMCSA with a more extended conjugation length, the corresponding wavelength for $S_0 \rightarrow S_1$ transition is red-shifted by 110 nm. The corresponding oscillator strength also increases from 1.33 to 1.43. There is also an appreciable increase in the excitation wavelength on moving from BMCSA to BPyMCSA, which could be attributed to the ICT in BPyMCSA. The corresponding oscillator strength increases from 1.43 to 3.17. In general, the excitation energy for the $S_0 \rightarrow S_1$ transition gradually decreases on moving down the series from BPCSA to BPyMCSA. Higher-energy electronic excitations for neutral precursors, except the $S_0 \rightarrow S_2$ transition in the BMCSA molecule, have insignificant oscillator strengths (not exceeding 0.1).

In comparison with the neutral precursors, one finds significant changes in the electronic structure of some of the cations. However, there is almost no such change on moving from the neutral precursors BPCSA and BPyMCSA to their respective cations. The excitation wavelengths of BPCSA/BPCSA+ and BPyMCSA/BPyMCSA+ are 321nm/318nm and 522nm/530nm respectively. Similarly, the oscillator strengths for the pairs are respectively 1.63/1.45 and 3.17/3.17. In contrast to this, we witnessed significant changes for the other two pairs. In one hand, the brightest one-photon state S_1 in NCSA becomes a dark state in NCSA+, whereas on the other hand, the dark one-photon state S_2 in NCSA becomes brightest in NCSA+. However, there is no significant change in excitation wavelengths. Interestingly, only for the BMCSA/BMCSA+ pair there is a significant red-shift of the first electronic transition (roughly by 60 nm), with a slight decrease in the oscillator strength. The second excited states in this pair is located almost at the same position relative to the ground state. It should be highlighted that the structural modification allows for red-shift of first intense transition roughly by 200 nm, e.g. on passing from NCSA to BPyMCSA. This result might be beneficial for construction of the active organic layer for PVSK with desired photophysical properties.

3.2 Two-photon absorption

The two-photon activity of an electronic system is measured in terms of its two-photon transition strength (δ_{0J}). Within the coupled-cluster theory the orientationally averaged δ_{0J} for a transition between states $|0\rangle$ and $|J\rangle$ is given as[40]

$$\langle \delta_{0J}^{\mathrm{2PA}} \rangle = \frac{1}{15} \sum_{\mu} \sum_{\nu} \left[M_{J\leftarrow 0}^{\mu\mu} M_{0\leftarrow J}^{\nu\nu} + M_{J\leftarrow 0}^{\mu\nu} M_{0\leftarrow J}^{\mu\nu} + M_{J\leftarrow 0}^{\mu\nu} M_{0\leftarrow J}^{\nu\mu} \right] \quad (1)$$

where $\mu, \nu \in x, y, z$. The symbols $M_{J\leftarrow 0}^{\mu\mu}$ and $M_{0\leftarrow J}^{\nu\nu}$ are used to denote right and left second-order transition moments, respectively. In the case of one source of photons, *i.e.*, $\omega = \frac{1}{2}\omega_J$, they read:

$$M_{0\leftarrow J}^{XY} = \sum_K \left(\frac{\langle 0|X|K\rangle\langle K|Y|J\rangle}{\frac{1}{2}\omega_J - \omega_K} + \frac{\langle 0|Y|K\rangle\langle K|X|J\rangle}{\frac{1}{2}\omega_J - \omega_K} \right) \quad (2)$$

$$M_{J\leftarrow 0}^{XY} = \sum_K \left(\frac{\langle J|X|K\rangle\langle K|Y|0\rangle}{\frac{1}{2}\omega_J - \omega_K} + \frac{\langle J|Y|K\rangle\langle K|X|0\rangle}{\frac{1}{2}\omega_J - \omega_K} \right) \quad (3)$$

The values of δ_{0J} calculated for the first five singlet excited states of all the four neutral precursors and their cations are also presented in Table 1 (see last column). The following two key observations can be drawn based on the analysis of the results presented therein for neutral precursors. Firstly, in the case of BPCSA, BMCSA and BPyMCSA molecules, the lowest-energy bright transitions with large values of oscillator strengths are connected with insignificant two-photon activity. However, some of the dark states in the one-photon absorption spectra of neutral precursors exhibit incomparably large two-photon transition strengths (and corresponding two-photon absorption cross sections). For NCSA, we note that the bright S_1 state exhibits the largest two-photon strength among its first five excited states. Secondly, the largest two-photon activity is found for symmetric molecules BPyMCSA (S_2, A symmetry) and BMCSA (S_3, A symmetry). The second largest two-photon strength is exhibited by the S_3 state in BMCSA. In order to analyze this behaviour, we have employed recently developed generalized few-state model (GFSM) for electronic structure theories with a non-hermitian structure.[33] GFSM allows to interpret the two-photon transition strengths in terms of electronic structure parameters:

$$\begin{aligned}
\langle \delta_{0J}^{\mathrm{GFSM}} \rangle &= \sum_K \sum_L \delta_{0JKL}^{\mathrm{GFSM}}, \quad \text{where} \\
\langle \delta_{0JKL}^{\mathrm{GFSM}} \rangle &= \frac{2}{15 \Delta E_K \Delta E_L} (\alpha + \beta), \quad (4) \\
\alpha &= |\mu^{JK}||\mu^{K0}||\mu^{0L}||\mu^{LJ}| \times \\
&\quad \left(\cos\theta_{JK}^{K0} \cos\theta_{0L}^{LJ} + \cos\theta_{JK}^{0L} \cos\theta_{K0}^{LJ} + \cos\theta_{JK}^{LJ} \cos\theta_{K0}^{0L} \right) \\
\beta &= |\mu^{JL}||\mu^{L0}||\mu^{0K}||\mu^{KJ}| \times \\
&\quad \left(\cos\theta_{JL}^{L0} \cos\theta_{0K}^{KJ} + \cos\theta_{JL}^{0K} \cos\theta_{L0}^{KJ} + \cos\theta_{JL}^{KJ} \cos\theta_{L0}^{0K} \right)
\end{aligned}$$

In the above expression (Eq. 4), the superscripts distinguish between the right ($L0$) and the left ($0L$) moments and $\Delta E_K = \frac{1}{2}\omega_J - \omega_K$. The term θ_{PQ}^{RS} represents the angle between the transition dipole moment vectors μ^{PQ} and μ^{RS}. Note that for the time-dependent density functional theory, in which case the left and right moments are equal, the above expression reduces to the one derived previously by one of the present authors.[41] The summation in Eq. 4 runs over all the electronic states. In principle, any number of intermediate states K and L can be chosen in Eq. 4. In the present study we employed a three-state model (3SM), in which K and L can be either the ground state 0, an intermediate or the final excited state

Table 1 Excitation energies (ΔE, eV), wavelengths (λ, nm), oscillator strengths (f) and two-photon transition strengths ($\langle\delta^{2PA}\rangle$, au.) for the transitions to the five lowest-lying singlet excited states. All results were obtained at the RI-CC2/cc-pVDZ level.

	Symmetry	ΔE (λ)	f	$\langle\delta^{2PA}\rangle\times10^3$
BPCSA	A (S_1)	3.86 (321)	1.63	4.6
	A (S_2)	4.62 (268)	0.02	1.0
	A (S_3)	4.67 (265)	0.01	2.7
	A (S_4)	4.91 (252)	0.07	97.9
	A (S_5)	5.02 (247)	0.00	0.1
BPCSA+	A (S_1)	3.896 (318)	1.45	12.9
	A (S_2)	4.584 (271)	0.01	<0.1
	A (S_3)	4.604 (269)	0.00	<0.1
	A (S_4)	4.646 (270)	0.00	4.6
	A (S_5)	4.923 (252)	0.20	86.5
NCSA	A (S_1)	3.76 (330)	1.33	25.6
	A (S_2)	4.01 (309)	0.00	<0.1
	A (S_3)	4.58 (271)	0.00	<0.1
	A (S_4)	4.61 (269)	0.01	0.3
	A (S_5)	4.69 (264)	0.00	1.1
NCSA+	A (S_1)	3.996 (310)	0.01	<0.1
	A (S_2)	4.153 (300)	1.35	3.1
	A (S_3)	4.527 (274)	0.00	<0.1
	A (S_4)	4.673 (265)	0.01	0.3
	A (S_5)	4.695 (264)	0.02	<0.1
BMCSA	B (S_1)	2.81 (441)	1.43	<0.1
	B (S_2)	3.49 (355)	0.62	<0.1
	A (S_3)	3.71 (334)	0.00	491.7
	A (S_4)	4.19 (296)	0.00	264.0
	B (S_5)	4.50 (275)	0.05	<0.1
BMCSA+	B (S_1)	2.467 (503)	0.66	<0.1
	B (S_2)	3.554 (349)	1.28	<0.1
	A (S_3)	3.716 (334)	0.00	524
	A (S_4)	4.372 (284)	0.00	64
	B (S_5)	4.546 (273)	0.02	0.2
BPyMCSA	B (S_1)	2.37 (522)	3.17	0.0
	A (S_2)	2.99 (415)	0.00	858.6
	B (S_3)	3.10 (401)	0.01	0.0
	A (S_4)	3.13 (396)	0.00	214.2
	A (S_5)	3.38 (367)	0.00	2.7
BPyMCSA+	B (S_1)	2.337 (530)	3.17	0.3
	A (S_2)	2.755 (450)	0.00	669.6
	B (S_3)	2.801 (443)	0.04	10.7
	A (S_4)	2.890 (429)	0.00	379.5
	B (S_5)	3.067 (404)	0.00	<0.1

Table 2 Two-photon transition strengths ($\langle\delta^{2PA}\rangle$, au.) predicted based on a three-state model including the ground state, the final and a key intermediate state.

	Initial state	Final state	Key intermediate state	$\langle\delta^{2PA}\rangle$ (3SM) $\times 10^3$
BPCSA	S_0	S_4	S_1	117.5
BMCSA	S_0	S_3	S_1	305.7
	S_0	S_4	S_1	276.3
BPyMCSA	S_0	S_2	S_1	985.4
	S_0	S_4	S_1	254.2

Table 3 Excitation energies (ΔE, eV), wavelengths (λ, nm), oscillator strengths (f) and dominant one-electron excitations between frontier orbitals for the transitions to the two lowest-lying singlet excited states. All results were obtained at the CAM-B3LYP/cc-pVDZ level of theory

	Symmetry	ΔE	f	orbital character
BPyMCSA	B (S_1)	2.318 (535)	2.70	HOMO→LUMO
	A (S_2)	3.083 (402)	0.00	HOMO→LUMO+1, HOMO→LUMO+2
BPyMCSA+	B (S_1)	2.132 (582)	1.10	HOMO→LUMO
	A (S_2)	2.184 (567)	0.00	HOMO→LUMO+1

J. Given $0 \rightarrow J$ transition, we performed three-state model calculations including all possible intermediate states within considered manifold of excited states (S_1-S_5). The summary of these calculations for BPCSA, BMCSA and BPyMCSA is shown in Table 2 (see the Electronic Supplementary Information for complete data). Both NCSA and its cation exhibit very low two-photon activity and hence we did not present the data for NCSA in this table. However, we noticed that for NCSA, a two-state model is sufficient to reproduce the response theory results. The other excited states in NCSA owing to having a very small transition dipole moments (either $\mu^{1K/K0}$ or $\mu^{0L/L1}$ or both) are inactive towards contribution to its two-photon activity. These data along with detailed GFSM data for other systems are supplied in the Electronic Supplementary Information file. It follows from the data presented in Table 2 that: i) for each electronic two-photon excitation with significant strength, the key intermediate state contributing to the two-photon activity is the brightest one-photon state, ii) the three-state model calculations satisfactorily reproduce the response-theory values reported in Table 1. Note that "the key intermediate state" is such state which makes the major contribution to the two-photon transition strength as defined by the sum-over-state expression (see Eq. 2–4). For example, in case of BMCSA and BPyMCSA, the contribution of the S_1 state (*i.e.* δ_{0J11} term) is 99.98% of the total δ_{0J} value obtained from the response theory. The second highest contribution comes from the cross terms $\delta_{0J01} = \delta_{0J10}$, which corresponds to a contribution of only 0.01% each. Similarly, in BPCSA the contributions of δ_{0J11} and δ_{0J14} are 92.47% and 3.58% respectively. The other terms have negligible contributions. A close scrutiny of the GFSM results indicates that the transition moments for $S_0 \rightarrow S_1$ and $S_1 \rightarrow S_{K/L}$ are significantly larger than the $S_0 \rightarrow S_{K/L}$ transition(s). This makes the contributions of δ_{0J11} and $\delta_{0JKL}, K \neq L \neq J$ much larger than that of other terms. Based on the GFSM results obtained for neutral precursors one may conclude that a further increase of two-photon transition strengths to the discussed electronic excitations might lead through modifications of properties of the S_1 electronic excited states (energy decrease, one-photon intensity increase). In fact, this strategy was utilized in chemical modifications BMCSA→BPyMCSA. Table 1 also contains the results of calculations of two-photon transition strengths for cations. In a qualitative sense, the two-photon spectra of cations shares the main features of spectra for neutral precursors, albeit we note some drop in the two-photon intensity for BPyMCSA+ (in comparison with BPyMCSA). Among all the studied cations, similarly to their neutral precursors, the largest two-photon transition strength is observed for BPyMCSA+ for the $S_0 \rightarrow S_2$ transition. The two-photon $S_0 \rightarrow S_2$ excitation wavelength is 900 nm, which is red-shifted in comparison with other studied cations. In order to better understand the nature of $S_0 \rightarrow S_1$ and $S_0 \rightarrow S_2$ excitations in the BPyMCSA/BPyMCSA+ pair, we performed additional electronic-structure calculations using the CAM-B3LYP functional and the cc-pVDZ basis set. The choice of TD-DFT is dictated by the fact, that in the linear-response coupled-cluster method, the transition vector does not describe the transition from one orbital to another. The electronic-structure parameters for these two electronic excitations, together with their orbital character, are shown in Table 3. As expected, the $S_0 \rightarrow S_1$ excitation is dominated by the HOMO→LUMO orbital transition. The HOMO orbital for BPyMCSA closely resembles the one for BPyMCSA+, and both are localized on the π-conjugated path (see Fig. 2). However, there is a significant difference in the LUMO orbital between BPyMCSA and BPyMCSA+. For the latter, the LUMO involves terminal NH_3^+ moieties. The analysis of third-

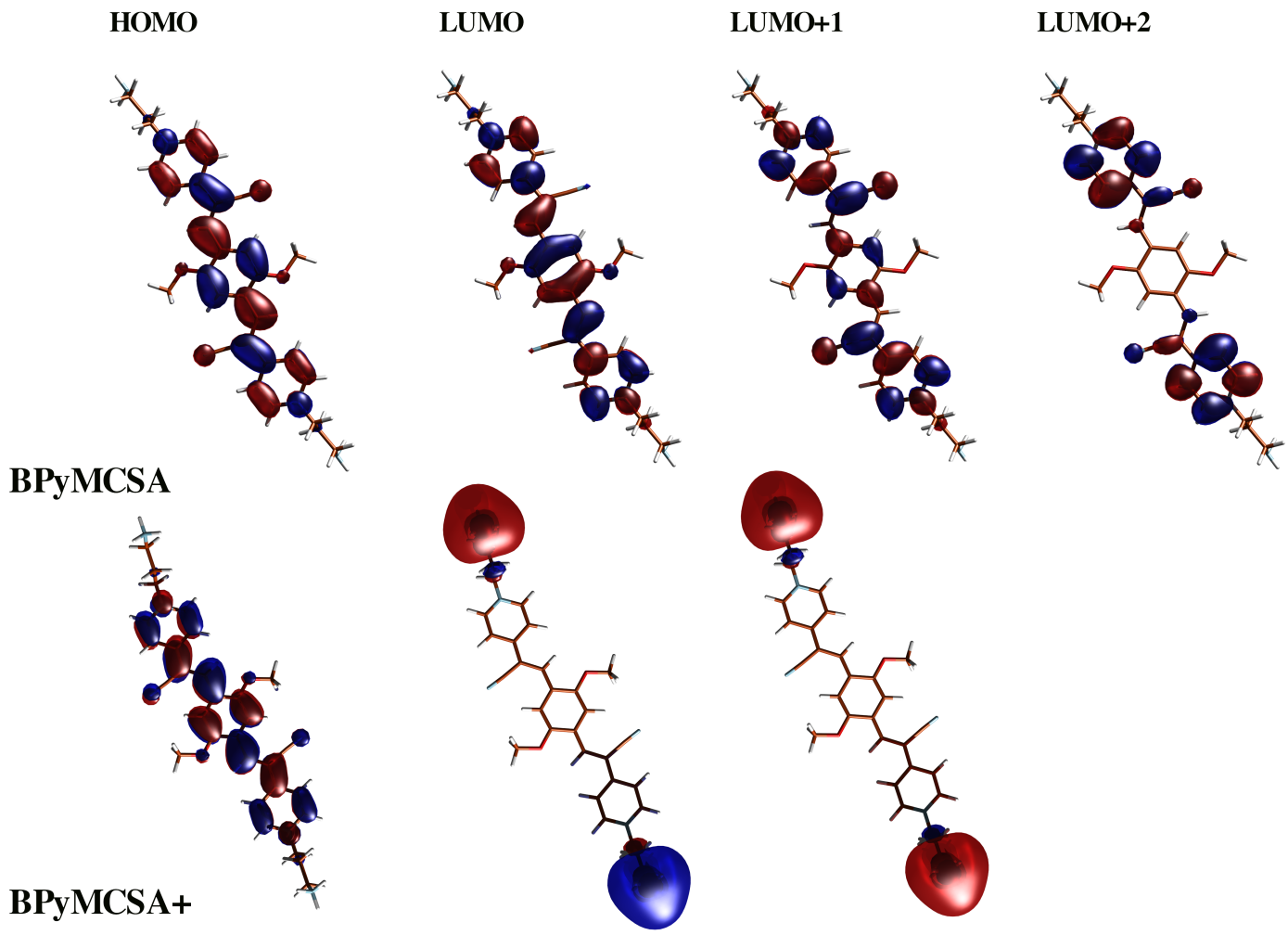

Fig. 2 Molecular orbitals involved in $S_0 \rightarrow S_1$ and $S_0 \rightarrow S_2$ electronic excitations for BPyMCSA and BPyMCSA+ molecules. See text for details.

order nonlinear optical properties for quadrupolar molecules has been a subject of numerous studies (see Ref. 42–47 and references therein). In particular, based on the proposed models, it is expected that quadrupolar structures will exhibit larger resonant third-order responses than their dipolar counterparts. These observations are in line with the results of the ab initio calculations presented in the present work, i.e. two-photon transition strengths for low-lying excited states are much larger for BMCSA and BPyMCSA than for NCSA. As highlighted by Terenziani *et al.* large TPA cross-sections are expected for dyes with intermediate quadrupolar character (defined in terms of the ρ parameter corresponding to the admixture of a neutral and a charged resonance form).[43] Thus, BMCSA and BPyMCSA can be a basis for further tuning of two-photon absorption properties by proposing structures with optimal ρ parameter. In conclusion, among the set of studied neutral precursors and their cations, the BPyMCSA/BPyMCSA+ pair exhibits the features desired for an organic active layer in PVSK, i.e. there is a low-lying state with an accompanying large two-photon transition strength and the corresponding two-photon excitation wavelength is in the infrared region.

4 Conclusions

In conclusion, with the aim to provide a design strategy for an effective photoactive layer in quasi-2D perovskite, in this work we study the one- and two-photon activity in four neutral organic precursors and their cations theoretically. The results obtained at the coupled-cluster level of theory (using CC2 model) indicate that two of the four neutral (cationic) precursors exhibit large two-photon activity. On moving from the neutral to the corresponding cationic form of the precursor named BMCSA, there is a significant bathochromic shift of the one-photon active state. Similarly on moving from the least two-photon active NCSA precursor to the most two-photon active BPyMCSA, there is a bathochromic shift of 200 nm. This result indicates that similar structural modification (as done for NCSA→BPyMCSA) can be used for construction of active organic layer for perovskite. The microscopic analysis based on three-state model reveals that the key excited state contributing to the two-photon activity in these compounds is the one that shows the highest one-photon activity. This in turn sug-

gests that the design of an effective organic photo-active layer in quasi-2D perovskite can be done by changing the electronic structure of the one-photon active state.

Acknowledgments: R.Z. gratefully acknowledges the support from the National Science Centre, Poland (Grant No. 2018/30/E/ST4/00457). M.M.A. thankfully acknowledges the "Research Initiation Grant (IIT Bhilai/D/2258)" provided by Indian Institute of Technology Bhilai. H.Å. and P.N.P. acknowledge the US Air Force of Scientific Research (contract FA-9550-18-1-0032 and FA-9550-18-1-0042) for support. The authors declare no competing financial interest.

References

1 D. A. Parthenopoulos and P. M. Rentzepis, *Science*, 1989, **245**, 843–845.
2 A. S. Dvornikov, E. P. Walker and P. M. Rentzepis, *J. Phys. Chem. A*, 2009, **113**, 13633–13644.
3 G. S. He, L.-S. Tan, Q. Zheng and P. N. Prasad, *Chem. Rev.*, 2008, **108**, 1245–1330.
4 W. Denk, J. Strickler and W. Webb, *Science*, 1990, **248**, 73–76.
5 A. M. Streets, A. Li, T. Chen and Y. Huang, *Anal. Chem.*, 2014, **86**, 8506–8513.
6 E. E. Hoover and J. A. Squier, *Nat. Photon.*, 2013, **7**, 93–101.
7 C.-Y. Chung, J. Boik and E. O. Potma, *Ann. Rev. Phys. Chem.*, 2013, **64**, 77–99.
8 K. A. Green, M. P. Cifuentes, T. C. Corkery, M. Samoc and M. G. Humphrey, *Angew. Chem. Int. Ed.*, 2009, **48**, 7867–7870.
9 F. Castet, V. Rodriguez, J.-L. Pozzo, L. Ducasse, A. Plaquet and B. Champagne, *Acc. Chem. Res.*, 2013, **46**, 2656–2665.
10 K. J. Chen, A. D. Laurent and D. Jacquemin, *J. Phys. Chem. C*, 2014, **118**, 4334–4345.
11 J. Boixel, V. Guerchais, H. Le Bozec, D. Jacquemin, A. Amar, A. Boucekkine, A. Colombo, C. Dragonetti, D. Marinotto, D. Roberto, S. Righetto and R. De Angelis, *J. Am. Chem. Soc.*, 2014, **136**, 5367–5375.
12 T. Jaunet-Lahary, A. Chantzis, K. J. Chen, A. D. Laurent and D. Jacquemin, *J. Phys. Chem. C*, 2014, **118**, 28831–28841.
13 M. Schulze, M. Utecht, A. Hebert, K. Rück-Braun, P. Saalfrank and P. Tegeder, *J. Phys. Chem. Lett.*, 2015, **6**, 505–509.
14 R. Swofford and A. Albrecht, *Annu. Rev. Phys. Chem.*, 1978, **29**, 421–440.
15 H. Mahr, in *Quantum Electronics - Nonlinear Optics, Part A*, ed. H. Rabin and C. L. Tang, Academic Press, New York, 1975, vol. 1.
16 N. Bloembergen, *Nonlinear optics*, World Scientific, 1996.
17 M. Albota, D. Beljonne, J.-L. Brédas, J. Ehrlich, J.-Y. Fu, A. Heikal, S. Hess, T. Kogej, M. Levin, S. Marder, D. McCord-Maughon, J. Perry, H. Röckel and M. Rumi, *Science*, 1998, **281**, 1653–1656.
18 T. Kogej, D. Beljonne, F. Meyers, J. Perry, S. Marder and J. Brédas, *Chem. Phys. Lett.*, 1998, **298**, 1–6.
19 F. Terenziani, C. Katan, E. Badaeva, S. Tretiak and M. Blanchard-Desce, *Adv. Mat.*, 2008, **20**, 4641–4678.
20 M. Pawlicki, H. A. Collins, R. G. Denning and H. L. Anderson, *Angew. Chem. Int. Ed.*, 2009, **48**, 3244–3266.
21 M. Göppert-Mayer, *Ann. Phys.*, 1931, **9**, 273–294.
22 W. Peticolas, J. Goldsborough and K. Rieckhoff, *Phys. Rev. Lett.*, 1963, **10**, 43–45.
23 W. Peticolas and K. Rieckhoff, *J. Chem. Phys.*, 1963, **39**, 1347–1348.
24 R. R. Birge, J. A. Bennett, B. M. Pierce and T. M. Thomas, *J. Am. Chem. Soc.*, 1978, **100**, 1533–1539.
25 H. J. Neusser and E. W. Schlag, *Angew. Chem. Int. Ed. Engl.*, 1992, **31**, 263–273.
26 M. Drobizhev, N. S. Makarov, S. E. Tillo, T. E. Hughes and A. Rebane, *Nat. Methods*, 2011, **8**, 393–399.
27 B.-G. Wang, K. König and K.-J. Halbhuber, *J. Microsc.*, 2010, **238**, 1–20.
28 C.-K. Lim, M. Maldonado, R. Zalesny, R. Valiev, H. Ågren, A. S. Gomes, J. Jiang, R. Pachter and P. N. Prasad, *Adv. Funct. Mater.*, 2020, 1909375.
29 A. D. Becke, *J. Chem. Phys.*, 1993, **98**, 5648–5652.
30 T. H. Dunning Jr., *J. Chem. Phys.*, 1989, **90**, 1007–1023.
31 C. Hättig and F. Weigend, *J. Chem. Phys.*, 2000, **113**, 5154–5161.
32 M. T. P. Beerepoot, D. H. Friese, N. H. List, J. Kongsted and K. Ruud, *Phys. Chem. Chem. Phys.*, 2015, **17**, 19306–19314.
33 M. T. P. Beerepoot, M. M. Alam, J. Bednarska, W. Bartkowiak, K. Ruud and R. Zaleśny, *J. Chem. Theory Comput.*, 2018, **14**, 3677–3685.
34 D. Jacquemin, V. Wathelet, E. A. Perpéte and C. Adamo, *J. Chem. Theory Comput.*, 2009, **5**, 2420–2435.
35 M. J. Frisch, G. W. Trucks, H. B. Schlegel, G. E. Scuseria, M. A. Robb, J. R. Cheeseman, G. Scalmani, V. Barone, G. A. Petersson, H. Nakatsuji, X. Li, M. Caricato, A. V. Marenich, J. Bloino, B. G. Janesko, R. Gomperts, B. Mennucci, H. P. Hratchian, J. V. Ortiz, A. F. Izmaylov, J. L. Sonnenberg, D. Williams-Young, F. Ding, F. Lipparini, F. Egidi, J. Goings, B. Peng, A. Petrone, T. Henderson, D. Ranasinghe, V. G. Zakrzewski, J. Gao, N. Rega, G. Zheng, W. Liang, M. Hada, M. Ehara, K. Toyota, R. Fukuda, J. Hasegawa, M. Ishida, T. Nakajima, Y. Honda, O. Kitao, H. Nakai, T. Vreven, K. Throssell, J. A. Montgomery, Jr., J. E. Peralta, F. Ogliaro, M. J. Bearpark, J. J. Heyd, E. N. Brothers, K. N. Kudin, V. N. Staroverov, T. A. Keith, R. Kobayashi, J. Normand, K. Raghavachari, A. P. Rendell, J. C. Burant, S. S. Iyengar, J. Tomasi, M. Cossi, J. M. Millam, M. Klene, C. Adamo, R. Cammi, J. W. Ochterski, R. L. Martin, K. Morokuma, O. Farkas, J. B. Foresman and D. J. Fox, *Gaussian 16 Revision B.01*, 2016, Gaussian Inc. Wallingford CT.
36 *TURBOMOLE V7.3 2018, a development of University of Karlsruhe and Forschungszentrum Karlsruhe GmbH, 1989-2007, TURBOMOLE GmbH, since 2007; available from*

http://www.turbomole.com.
37 M. Barzoukas and M. Blanchard-Desce, *J. Chem. Phys.*, 2000, **113**, 3951–3959.
38 D. B. Mitzi, *J. Chem. Soc., Dalton Trans.*, 2001, 1–12.
39 B.-K. An, J. Gierschner and S. Y. Park, *Acc. Chem. Res.*, 2012, **45**, 544–554.
40 D. H. Friese, C. Hättig and K. Ruud, *Phys. Chem. Chem. Phys.*, 2012, **14**, 1175–1184.
41 M. M. Alam, M. Chattopadhyaya and S. Chakrabarti, *Phys. Chem. Chem. Phys.*, 2012, **14**, 1156–1165.
42 S. Hahn, D. Kim and M. Cho, *J. Phys. Chem. B*, 1999, **103**, 8221–8229.
43 F. Terenziani, A. Painelli, C. Katan, M. Charlot and M. Blanchard-Desce, *J. Am. Chem. Soc.*, 2006, **128**, 15742–15755.
44 J. Zyss and I. Ledoux, *Chem. Rev.*, 1994, **94**, 77–105.
45 M. Barzoukas and M. Blanchard-Desce, *J. Chem. Phys.*, 2000, **113**, 3951–3959.
46 A. Kovalenko, M. Vala, M. Ciganek, M. Weiter and J. Krajcovic, *Chem. Pap.*, 2018, **72**, 3033–3042.
47 B. Mettra, T. Le Bahers, C. Monnereau and C. Andraud, *Dyes Pigments*, 2018, **159**, 352–366.